

Experimental evidence of the kinetic performance achievable with columns packed with the new 1.9 μm fully porous particles Titan C₁₈.

Omar Ismail^a, Martina Catani^b, Luisa Pasti^b, Alberto Cavazzini^{b,*}, Alessia Ciogli^a, Claudio Villani^a, Dorina Kotoni^{a,c}, Francesco Gasparrini^{a,**}, David S. Bell^d

^a*Dept. of Drug Chemistry and Technology, "Sapienza" Università di Roma, P.le A. Moro 5, 00185 Roma, Italy*

^b*Dept. of Chemistry and Pharmaceutical Sciences, University of Ferrara, via L. Borsari 46, 44121 Ferrara, Italy*

^c*Current address: Chemical and Analytical Devel., Novartis Pharma AG, St. Johann Campus, 4102 Basel, Switzerland*

^d*Analytical Research and Services. Sigma-Aldrich/Supelco, 595 North Harrison Road. Bellefonte, PA 16823, USA*

Abstract

Six columns of different geometries (2.1 and 3.0 internal diameter \times 50, 75 and 100 mm length) packed with the new 1.9 μm fully porous Titan C₁₈ particles (80 Å pore size) have been tested under typical reversed phase conditions by employing a mixture of benzene derivatives as probes. The columns exhibited excellent kinetic performance with apparent estimated efficiencies in the order of 300,000 theoretical plates per meter. The minimum reduced HETP, h_{min} , was found as small as 1.7 at reduced velocities, ν , of roughly 8. Remarkably, the C -branch of the van Deemter equation was found to be very flat. This allowed for the use of the columns at relatively large flow rates without dramatically losing performance. For instance, on the 50 \times 2.1 mm column, it was found $h = 2.85$ at $\nu = 22.5$.

Keywords: Column efficiency, Sub-2 μm fully porous particles, Ultra High Performance Liquid Chromatography (UHPLC)

*Corresponding author

**Corresponding author

Email addresses: cvz@unife.it (Alberto Cavazzini), francesco.gasparrini@uniroma1.it (Francesco Gasparrini)

1. Introduction

During the last years, many efforts have been done to prepare chromatographic columns able to provide very high efficiency and large sample resolution in short times. This trend has led column manufacturers to produce shorter, narrower columns packed with finer particles. The use of sub- $2\mu\text{m}$ fully porous particles essentially reflects the need to improve mass transfer inside the column by reducing intraparticle diffusion (less steep C -term in the van Deemter equation), albeit at cost of increased back pressure to push fluid through the packed bed [1, 2]. However, the availability of fine particles is not enough for the preparation of columns suitable for high or ultra-high performance liquid chromatography (HPLC, UHPLC). The packing procedure and the column bed consolidation (shortly, the packing protocol) are indeed of utmost importance for optimal results. Pressurized slurry column packing is influenced by many variables that dramatically affect how good the column will perform in terms of efficiency and stability [3]. Some of the most important things to consider are: filling pressure; mode of operation (constant pressure versus constant flow, upflow versus downflow column filling); slurry liquid and concentration; effect of frictional and cohesive forces between small particles; packing particle characteristics (e.g, particle roughness, density, etc.); type of column inlet and outlet frit; bed compression techniques. In addition, it is well known that even particles of similar chemistry (very) often require completely different packing conditions to be efficiently packed into chromatographic columns (we need only think of the example of C_{18} fully porous vs. C_{18} core-shell particles to understand how this can be important). Not to say about particles of different chemistry that require, every time they are synthesized, the development of a new column packing method specific for that phase. For all these reasons, packing columns is still considered an art more than a science, whose results are hard to predict. Recently, columns packed with new $1.9\ \mu\text{m}$ fully porous spherical particles (nominal pore size $80\ \text{\AA}$) have been introduced into the market (commercial name: Titan C_{18} particles, from Supelco). Titan C_{18} particles are characterized by an unusually narrow particle size distribution (PSD) for fully porous particles, with a relative standard deviation (RSD) smaller than 10%. This is due to an innovative and proprietary

process for synthesizing fully porous spherical particles that, in addition, does not need from
30 any secondary sizing operation [4]. Usually, fully porous sub 2- μm particles come in broader
PSD, with RSD in the order of 20-25%. Therefore, in terms of PSD, Titan C₁₈ particles are
closer to core-shell particles, whose RSD is only approx. 5% due to the fact that they are
synthesized under conditions that allow for the accurate control of both the size of the solid
core and the thickness of the porous shell.

35 The most advanced study aimed at investigating the influence of PSD on column perfor-
mance are those based on the simulation of fluid flow and advective-diffusive mass transport
in the packing interparticle void space of computer-reconstructed bulk packings (as to avoid
the effect of different packing protocols on the final bed structure), performed by Tallarek
and coworkers [5–8]. They have shown that, as long as the PSD is reasonably narrow (RSD
40 \simeq 20-25%), the effect of PSD on chromatographic bulk dispersion is negligible, especially
if compared to that of the interstitial bed porosity [5, 6]. The morphological analysis of
physically reconstructed packings has shown indeed that the actual disorder in the bulk of
beds made of particles with narrow PSD is essentially the same as that found in beds packed
with particles of wide PSD [7, 8]. On the other hand, what makes the difference in terms
45 of kinetic performance in confined packings (e.g., chromatographic columns) are the wall
effects, which depend on the packing protocol and on the particle properties (including thus
their PSD).

The first detailed reports on the use of Titan C₁₈ columns in reversed phase liquid chro-
matography (RPLC) have evidenced their excellent kinetic performance [9, 10]. Extremely
50 low reduced plate heights, h_{min} , were found for retained compounds with values as small
as 1.7-1.9 [9, 10]. This is a rather exceptional observation by considering that, for columns
packed with fully porous particles, a minimum reduced plate height around 2 is (empiri-
cally) considered the limit representing a very well packed, homogeneous bed structure (on
the other hand, h_{min} values smaller than 1.6 are not uncommon for analytical-scale columns
55 packed with core-shell particles) [1, 8, 11–13]. Gritti and Guiochon [9, 10] employed a series
of phenone derivatives under RP conditions as probe compounds to investigate in detail all

the terms of the van Deemter equation. According to their study, Titan C₁₈ columns perform so well as they are characterized by an extremely small B -term, due to the very small intra-particle diffusivity across the Titan C₁₈ particles [10]. The internal obstruction factor, which
60 accounts for the overall diffusion hindrance in the confined pore geometry [14], was indeed found to be roughly 3 times smaller (for a retention factor of about 2) than for typical fully porous particles of similar chemistry. This explains also why the reduced optimum flow rate, ν_{opt} , was found at only around 4-5, while in RPLC it is usually around 10. The downside of a small B term is indeed a large C term in the van Deemter equation.

65 In this work, we report on the experimental evaluation of the kinetic behavior of 1.9 μm C₁₈ Titan columns. Essentially, we have measured van Deemter curves of a series of benzene derivatives up to the maximum back pressure allowed by our equipment (roughly 1,000 bar or 14,500 psi) on six columns with different geometrical characteristics. This is, in our opinion, a significant number of case studies to draw reliable conclusions. Our results are
70 surprising in the sense that if, on the one hand, we have also observed very low h_{min} values (essentially comparable to those reported in [9, 10]), on the other hand, we have not found the same steep dependence of the C -branch of the van Deemter equation on the mobile phase velocity. On the contrary, the van Deemter curve remained very flat up to the maximum flow rate achievable with our equipment (able to provide a maximum back-pressure of roughly
75 1,000 bar) and the h_{min} values were found at optimal reduced velocities of 8-10. This finding represents a major difference from the conclusions drawn in [9, 10], as it shows that these columns can be efficiently used also at high flow rates. In the companion paper to this one, we present a detailed study of the single terms of the van Deemter equation to understand their relative contribution to mass transfer of benzene derivatives across Titan C₁₈ columns.

80 2. Experimental section

Columns and materials. The six stainless steel Titan C₁₈ columns packed with 1.9 μm particles (80Å pore size; C₁₈ ligand density: 2 $\mu\text{mol}/\text{m}^2$; specific surface area: 400 m^2/g) were generously donated by Supelco Analytical (USA). Their dimensions (length \times internal-diameter, i.d.) were: 100 \times 2.1 mm, 75 \times 2.1 mm, 50 \times 2.1 mm, 100 \times 3.0 mm, 75 \times 3.0 mm and

85 50×3.0 mm. A 33×4.6 mm Micra column (Eprogen, Inc., USA) packed with 1.5 μm non-porous silica particles was purchased by DBA Italia s.r.l. (Italy). This column was employed for the estimation of bulk molecular diffusion coefficients. Uracil, phenol, nitrobenzene, benzaldehyde, benzene, toluene, ethylbenzene, butylbenzene, propylbenzene, pentylbenzene and tetrahydrofuran were purchased from Sigma-Aldrich. The fourteen polystyrene stan-
90 dards (molecular weights 500, 2000, 2500, 5000, 9000, 17500, 30000, 50000, 156000, 330000, 565000, 1030000, 1570000, 2310000), employed for Inverse Size Exclusion (ISEC) measurements, were from Supelco. Acetonitrile (ACN) was from VWR International and ultra-high quality Milli-Q water was obtained by a Milli-Q water purification system (Millipore).

Equipment. A Waters Acquity UPLC, controlled by Empower 3 software and equipped with
95 a binary solvent delivery system, an autosampler, a column thermostat, a photodiode array detector with a 500 nL cell, was used for the determination of the van Deemter curves. The equipment was operated under still-air conditions [15, 16]. The maximum back pressure reachable by the system is 1,000 bar. To reduce the extra-column contributions, two 250×0.075 mm nano-Viper capillary tubes (Thermo Scientific) were used to connect the
100 injector to the column and the column to the detector. The extra column peak variance, measured from the injector needle port to the detector cell, was 1.2 μL^2 (calculated through peak moments) at a flow rate of 1 mL/min (more details can be found as Supplementary Material). ISEC experiments were carried out on an Agilent 1100 Series Capillary LC system equipped with a binary pump system, an autosampler, a column thermostat (Peltier
105 unit) and a photodiode array detector. This equipment was also employed for peak parking experiments.

Inverse size exclusion chromatography ISEC measurements were performed by using tetrahydrofuran as the mobile phase [17]. Injection volume, flow rate and detection wavelength were, respectively, 2 μL , 0.1 mL/min and 254 nm. For ISEC plots (see later on), retention vol-
110 umes were corrected for the extra-column contribution before being plotted against the cubic root of the molecular weight (MW). Extra-column peak variance was calculated as the second central moment of the peak fitted through an exponentially modified Gaussian (EMG)

function [18].

Peak parking measurements. The flow rate used for peak parking measurements was 0.1 mL/min. Parking times were 0, 120, 600, 1200 and 1800 s. For the calculation of σ_x^2 , N was automatically processed by the integration tool of the software. All the data were corrected for the extra-column peak variance (see before).

Van Deemter curve measurements. For all columns, the van Deemter curves for nitrobenzene, toluene, ethylbenzene and butylbenzene were measured at $35\pm 1^\circ\text{C}$. The mobile phase was a binary mixture of ACN/water 60:40 v/v. The injection volume was $0.5\ \mu\text{L}$. Retention time and column efficiency of eluted peaks were automatically calculated by the integration process of the Empower 3 software. The detection wavelength was 214 nm; sampling rate was 80 points/s. Due to the very reduced extra-column volume of the modified Waters UPLC employed in this work (see before), no correction was necessary to compensate for the extra-column contribution (admittedly, for the 50×2.1 mm column, extra-column contribution represents 3-5% of column variance). The flow rates employed for studying the dependence of H on the mobile phase velocity were 0.025, 0.05, 0.1 ml/min and then, from 0.1 ml/min to the maximum reachable flow rate with step increments of 0.1 ml/min (see figure captions for more information).

130 3. Discussion

A detailed characterization of geometrical and physico-chemical characteristics of all the columns used in this work has been done through a series of measurements combining ISEC, pycnometry, peak parking and the traditional study of the dependence of the efficiency on the flow rate (van Deemter curves) [19, 20].

ISEC experiments. Figure 1 reports the ISEC plot for the estimation of interstitial and thermodynamic void volumes [21], measured on the 75×3.0 mm Titan C_{18} column. The interstitial volume, V_e , was derived from the extrapolation to $MW = 0$ of the linear regression calculated for the volumes of the totally excluded polystyrene samples. From this, the

estimation of external column porosity, ϵ_e , is straightforward (being $\epsilon_e = V_e/V_{col}$, with V_{col}
 140 the geometric volume of the column). The ISEC estimation of the thermodynamic void
 volume, V_0 , was based on the retention volume of benzene. Through this, the total porosity
 ϵ_t can be calculated ($\epsilon_t = V_0/V_{col}$). Thus the particle porosity, ϵ_p , is given by [22]:

$$\epsilon_p = \frac{\epsilon_t - \epsilon_e}{1 - \epsilon_e} \quad (1)$$

The porosities (ϵ_t , ϵ_e , ϵ_p) for the six Titan C₁₈ columns are reported in Table 1. As it
 can be noticed, the estimates of ϵ_t , ϵ_e , ϵ_p from the six columns are remarkably consistent
 145 with each other. Their average values are $\epsilon_t = 0.603 \pm 0.009$, $\epsilon_e = 0.371 \pm 0.009$ and
 $\epsilon_p = 0.368 \pm 0.007$ (errors are reported as plus/minus one standard deviation). For all
 columns, the thermodynamic void volume was estimated also by pycnometry. The agreement
 between void volumes estimated by ISEC and pycnometry was reasonably satisfactory in
 all cases (with differences in the order of roughly $\pm 5\%$). The pycnometric procedure and
 150 obtained void volumes are reported as Supplementary Material.

Estimation of molecular diffusion coefficients. Molecular diffusion coefficients, D_{ms} , were
 evaluated through the peak parking technique by employing a column packed with nonporous
 particles (Micra column). The procedure is well known (see further on) [13, 23, 24]. The peak
 parking method permits the empirical estimation of the apparent (or effective) axial diffusion
 155 coefficient in the composite material made of porous particles in contact and dispersed in
 the eluent matrix, D_{eff} . For columns packed with nonporous particles:

$$D_{eff} = \gamma_e D_m \quad (2)$$

where γ_e is the external obstruction factor generated by the tortuosity and constriction of
 inter-particle channels [14]. Accordingly, if γ_e is known, D_m can be calculated by:

$$D_m = \frac{D_{eff}}{\gamma_e} \quad (3)$$

The value of γ_e (D_{eff}/D_m) was determined by measuring D_{eff} (by means of peak parking)
 160 for a molecule of known D_m . In this work, thiourea in pure water at 25°C was used (under

these conditions, D_m of thiourea is 1.33×10^{-5} cm²/s) [25]. γ_e for the 33×4.6 mm Micra column was 0.68.

The peak parking method consists of: (1) taking at a constant, arbitrary linear velocity a sample zone somewhere in the middle of the chromatographic column; (2) suddenly stopping the flow; (3) leaving the band free to diffuse during a certain parking time, t_p ; (4) resuming the flow rate to move the band out of the column. The variance (in length units) of the eluted peak, σ_x^2 , is measured ($\sigma_x^2 = L^2/N$, where L is the column length and N the number of theoretical plates) and the procedure is repeated (keeping constant the flow rate) for different parking times. The slope of σ_x^2 vs. t_p plot gives an estimate of the D_{eff} , being [13, 24]:

$$D_{eff} = \frac{1}{2} \frac{\Delta\sigma_x^2}{\Delta t_p} \quad (4)$$

As an example, Figure 2 shows the σ_x^2 vs. t_p plot, employed for the estimation of D_{eff} (eq. 4), obtained for ethylbenzene. D_m of nitrobenzene, toluene, ethylbenzene and butylbenzene in ACN/H₂O 60/40 v/v at 35°C are reported in Table 2. As it can be seen from this Table, D_m values of alkyl-benzenes decrease quasi-linearly with increasing the number of methyl groups in the alkyl chain (from one to three), inasmuch as diffusion coefficients decrease with increasing the molecular size [26].

Specific permeability and Kozeny-Carman constant. The specific permeability of each column was calculated according to the traditional equation [12, 14]:

$$k_0 = \frac{u_s \eta L}{\Delta P} \quad (5)$$

where $u_s = F_v / \pi r_c^2$ is the superficial velocity (being r_c the inner column radius and F_v the flow rate in ml/min) and η the viscosity of the eluent ($\eta = 0.59$ cP for ACN/water 60/40, v/v) at 35°C. ΔP is the difference between the total pressure drop, P_{tot} , and the extra-column pressure drop, P_{ex} (P_{ex} was measured by replacing the column with a zero-volume connector). Experimentally, k_0 can be estimated by the slope of ΔP vs. u_s plot. Some examples of these plots for the columns used in this work are reported as Supplementary Material.

The Kozeny-Carman constant K_c was estimated by [12]:

$$K_c = \frac{\epsilon_e^3}{(1 - \epsilon_e)^2} \frac{d_p^2}{k_0} \quad (6)$$

where d_p is the particle size. For the calculation of K_c for Titan C₁₈ columns, the mean Sauter diameter d_{Sauter} was used (in place of the nominal $d_p = 1.9\mu\text{m}$). d_{Sauter} is indeed considered the most suitable average particle size to investigate sample dispersion along beds packed with non-uniform size distribution [27]. d_{Sauter} is defined by [28]:

$$d_{Sauter} = \frac{\sum n_i d_i^3}{\sum n_i d_i^2} \quad (7)$$

190 where d_i and n_i are, respectively, a given particle size and the number of particles with diameter included between d_i and $d_i + \Delta d_i$ (Δd_i was assumed $0.015\mu\text{m}$ for d_i values around $1\mu\text{m}$ and $0.25\mu\text{m}$ for d_i around $15\mu\text{m}$). d_{Sauter} was calculated at Supelco on some 30,000 particles. Its value was $2.04\mu\text{m}$ [9]. k_0 and K_c for all the considered columns values are listed in Table 1.

195 *Kinetic performance of Titan C₁₈ columns.* Figures 3 and 4 show the van Deemter plots obtained for the four compounds considered in this work on the two 50 mm Titan C₁₈ columns (3.0 and 2.1 mm i.d.). Other examples of van Deemter curves for columns of different geometries are reported as Supplementary Material. In these graphs, H is plotted as a function of the interstitial velocity, u_e :

$$u_e = \frac{F_v}{\pi r_c^2 \epsilon_e} \quad (8)$$

200 that is the average velocity of the mobile phase that moves between the particles [12]. From these plots, two common features can be evidenced. The first one is the very small value of the minimum H . For example, values as low as $H_{min} = 3.5\mu\text{m}$ (flow rate 0.6 ml/min, toluene compound) and $H_{min} = 3.4\mu\text{m}$ (flow rate 0.9 ml/min) were found for the 50×2.1 and the 50×3.0 mm columns, respectively. The second important aspect is that the so-called
 205 C -branch of the van Deemter curve is remarkably flat. For the cases reported in figs. 3 and 4, for example, at the maximum flow rates, the estimated H values were 4.0 (column 3.0×50

mm, $u_e = 1.2$ cm/sec, $F_v = 1.8$ ml/min) and $5.5 \mu\text{m}$ (column 2.1×50 mm, $u_e = 2.1$ cm/sec, $F_v = 1.6$ ml/min). Analogous behavior was observed also for the other Titan C₁₈ columns (see Supplementary Material for the van Deemter plots of the other columns).

210 Switching to reduced (or dimensionless) coordinates is a common way to compare packed beds of spherical particles [13, 14, 29]. Thus, all the next van Deemter curves are given in reduced coordinates, where the reduced velocity h :

$$h = \frac{H}{d_p} \quad (9)$$

is plotted against the reduced interstitial velocity ν :

$$\nu = \frac{u_e d_p}{D_m} \quad (10)$$

with D_m estimated through peak parking on a nonporous column (see before and Table 2).

215 The reduced van Deemter curves of the 50 mm columns (3.0 and 2.1 mm i.d.) are presented in Fig. 5, where for the sake of comparison we decided to show the plots obtained by using both the nominal particle diameter ($d_p = 1.9 \mu\text{m}$) and the Sauter diameter ($d_{Sauter} = 2.04 \mu\text{m}$). By assuming $d_p = 1.9 \mu\text{m}$, the minimum reduced plate height was found to be $h_{min} = 1.86$ at $\nu_{opt} = 7.1$ (50×3.0 mm column) and $h_{min} = 1.92$ at $\nu_{opt} = 7.9$ (50×2.1 mm column). On the
 220 other hand, if h is calculated by means of d_{Sauter} , the following values are obtained: $h_{min} = 1.73$ at $\nu_{opt} = 7.7$ (50×3.0 mm column) and $h_{min} = 1.79$ at $\nu_{opt} = 8.5$ (50×2.1 mm column). Remarkably, at the maximum $\nu = 12.5$ and 22.5 , respectively for the 50×3.0 mm and the 50×2.1 mm columns, the d_{Sauter} -based h values were only 2.03 and 2.85, showing how these columns do not dramatically loose efficiency by increasing the flow rate over its optimum
 225 value.

The reduced (d_{Sauter} -based) van Deemter plots for the two 75 mm and the two 100 mm columns are given in Fig. 6. As expected, these curves nearly superimpose (so do the reduced van Deemter curves of Fig. 5, not shown in this figure). To show up the great kinetic performance of the Titan C₁₈ columns, able to generate some 300,000 N/m at
 230 the optimum flow rate, Fig. 7 shows the chromatogram for the separation of a mixtures of benzene derivatives (phenol, benzaldehyde, nitrobenzene, benzene, toluene, ethylbenzene,

propylbenzene, butylbenzene, pentylbenzene with retention factor k ranging from 1 to almost 28) obtained on the 75×3.0 mm Titan C₁₈ column (see Figure caption for details). Under the Supplementary Material, a series of chromatograms for the separation of the same mixture
235 of compounds obtained with the other Titan C₁₈ columns are reported.

4. Conclusions

This study has confirmed that the Titan C₁₈ columns packed with the new 1.9 μm fully porous C₁₈ particles exhibit excellent kinetic performance under RP conditions. At their optimal flow rates, indeed, these columns were able to generate some 300,000 theoretical
240 plates per meter (with a retention factor of 4) by using a series of benzene derivatives as test compounds. The most important difference between our study and previous investigations on the same columns [9, 10] is in the high-velocity regime of van Deemter curve. Indeed, we have found that this region is not very sensitive to the mobile phase velocity. This therefore contrasts the findings of Gritti and Guiochon [9, 10], who report about a dramatic loss of
245 performance when columns are operated at reduced velocity larger than 5 (they used a series of phenone derivatives in RPLC), due to the extremely low intraparticle diffusivity across the Titan C₁₈ particles.

Contrary to this, not only have we observed that the optimal reduced velocities for the Titan C₁₈ column are quite comparable to that of columns packed with conventional fully
250 porous C₁₈ particles used in RP liquid chromatography ($\nu_{opt} = 8-10$), but also that the slope of the van Deemter equation remains very flat at high velocities. As a consequence, the Titan C₁₈ columns perform very well at reduced velocity larger than 15-18. In the companion paper to this one, we will present the results of the detailed study on the different contributions to mass transfer within Titan C₁₈ columns with the aim of understanding the rationale behind
255 their great performance.

5. Acknowledgments

The authors thank the Italian University and Scientific Research Ministry (Grant PRIN 2012ATMNJ.003) and the Laboratory Terra&Acqua Tech, member of Energy and Environ-

ment Cluster, Technopole of Ferrara of Emilia- Romagna High Technology Network. Dr.
260 Valentina Costa from the University of Ferrara is acknowledged for technical support.

6. Figures and Tables

Figure captions

Fig 1. ISEC plot. Retention volume (V_R) of polystyrene standards are plotted as a function of the cubic root of their molecular weight ($MW^{1/3}$). Column: Titan C₁₈ 75×3.0 mm. V_e :
265 interstitial volume; V_0 : thermodynamic void volume. See text for more details.

Fig 2. Peak parking experiments. Plot of band spreading (spatial peak variance, σ_x^2) as a function of the peak parking time, t_p (linear regression coefficient $R^2 > 0.99$).
270 1.5 μm nonporous silica particles. Compound: ethylbenzene; Mobile phase: ACN/water 60:40 v/v; T = 35°C; Column: Micra 33×4.6 mm,

Fig 3. Van Deemter plots of the plate height, H , vs. the interstitial linear velocity, u_e , for the Titan C₁₈ 50×3.0 mm. Experimental points: nitrobenzene (cyan), toluene (orange), ethylbenzene (green), butylbenzene (purple). The maximum u_e corresponds to a flow rate
275 F_v : 1.8 mL/min (system back-pressure: 646 bar; column back-pressure: 410 bar). (For interpretation of references to colours in this figure, readers are referred to the web version of the article).

Fig 4. Van Deemter plots of the plate height, H , vs. the interstitial linear velocity, u_e ,
280 for the Titan C₁₈ 50×2.1 mm. Experimental points: nitrobenzene (cyan), toluene (orange), ethylbenzene (green), butylbenzene (purple). The maximum u_e corresponds to a flow rate F_v : 1.6 mL/min (system back-pressure: 951 bar; column back-pressure: 743 bar). (For interpretation of references to colours in this figure, readers are referred to the web version of the article).

285

Fig 5. d_p -based (black points) and d_{Sauter} -based (red triangles) reduced van Deemter plots (h vs. ν) for the Titan C₁₈ 50×3.0 (top) and 50×2.1 (bottom) columns. (For interpretation

of references to colours in this figure, readers are referred to the web version of the article).

290 **Fig 6.** d_{Sauter} -based reduced van Deemter plots (h vs. ν) for the two 100 mm and the two 75 mm Titan C₁₈ columns. Columns: 100×3.0 mm (black); 75×3.0 mm (red); 100×2.1 mm (green); 75×2.1 mm (cyan). (For interpretation of references to colours in this figure, readers are referred to the web version of the article).

295 **Fig 7.** Chromatogram showing the separation of a mixture of benzene derivatives on the Titan C₁₈ 75×3.0 mm column. **Flow rate: 0.9 mL/min. Mobile** phase: ACN/water 60:40, v/v; T=35°C. Compounds: 1. Uracil (258933 N/m, $k = 0$); 2. Phenol (300280, $k = 0.8$); 3. Benzaldehyde (308680 N/m, $k = 1.3$); 4. Nitrobenzene (314160 N/m, $k = 1.9$); 5. Benzene (301000 N/m, $k = 2.8$); 6. Toluene (296200 N/m, $k = 4.3$); 7. Ethylbenzene (286720
300 N/m, $k = 6.5$); 8. Propylbenzene (271107 N/m, $k = 10.6$); 9. Butylbenzene (256733 N/m, $k = 17.1$); 10. Pentylbenzene (236920 N/m, $k = 27.7$). The retention factor k was calculated by using uracil as void time marker.

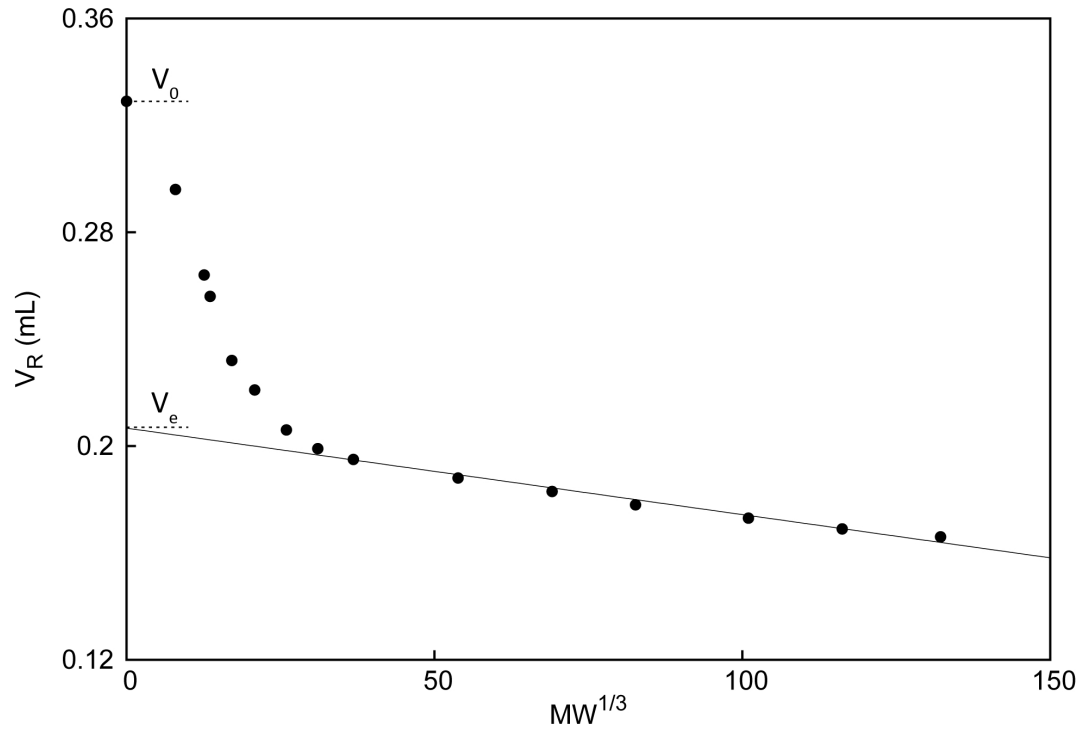


Figure 1:

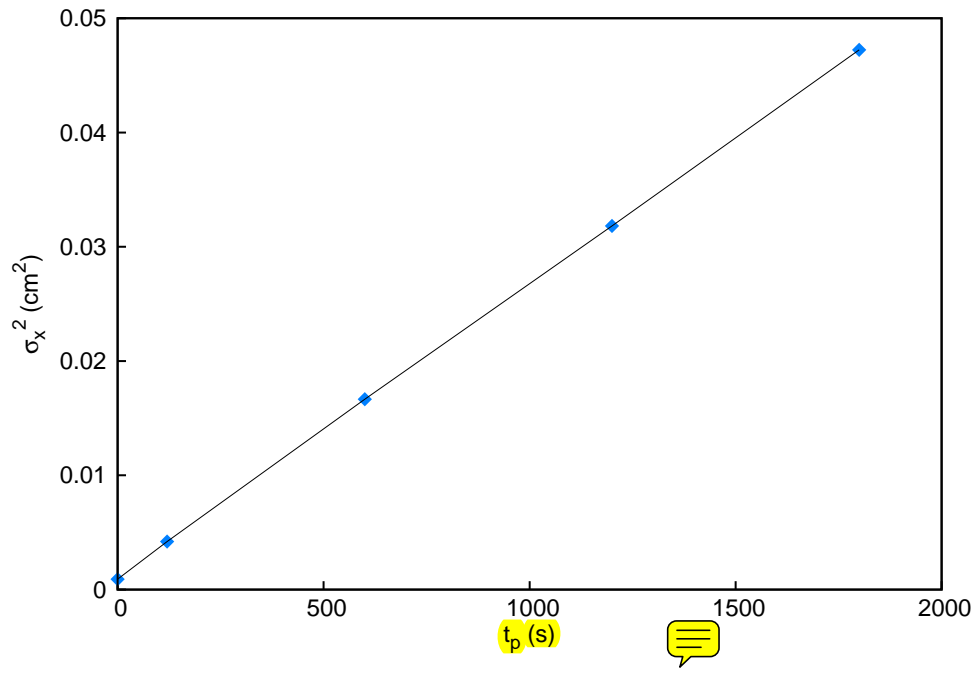


Figure 2:

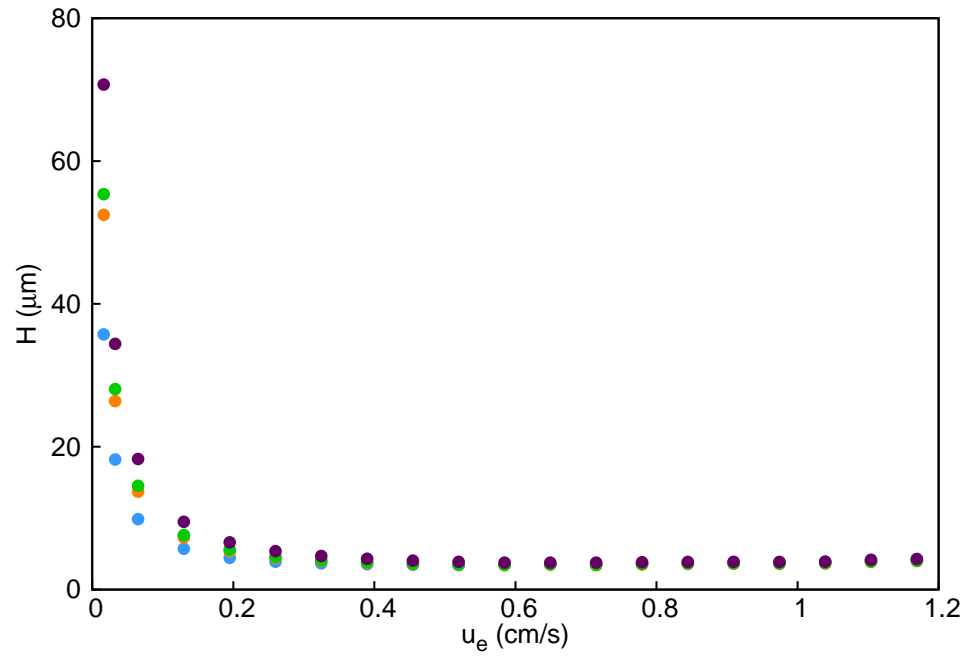


Figure 3:

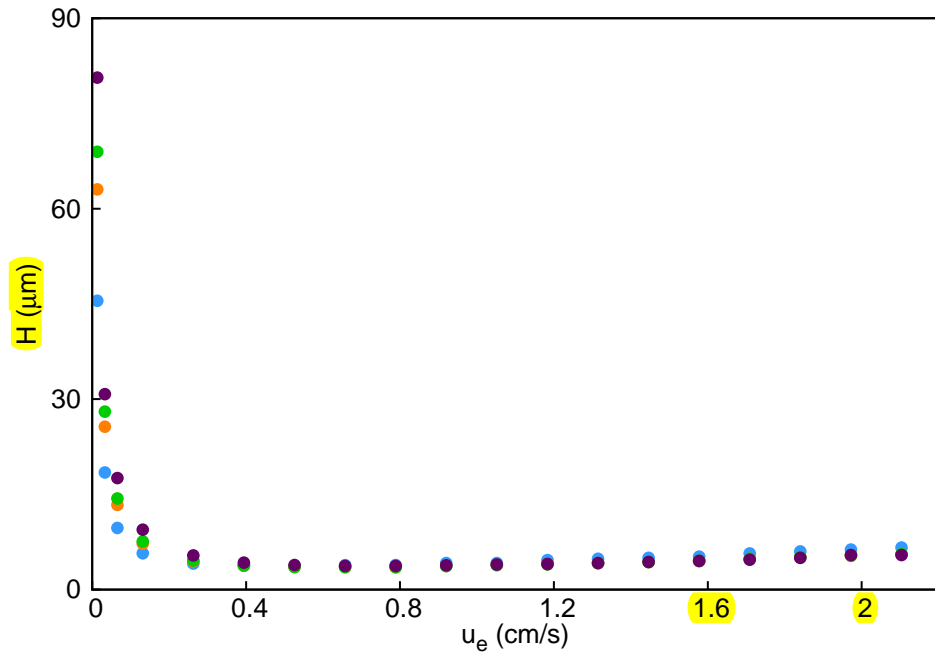


Figure 4:

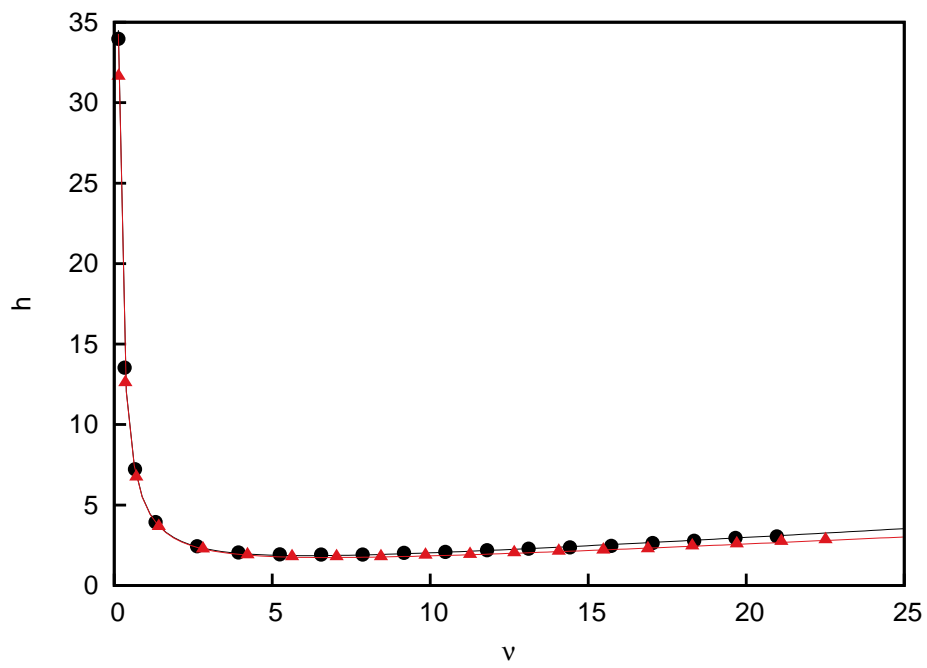
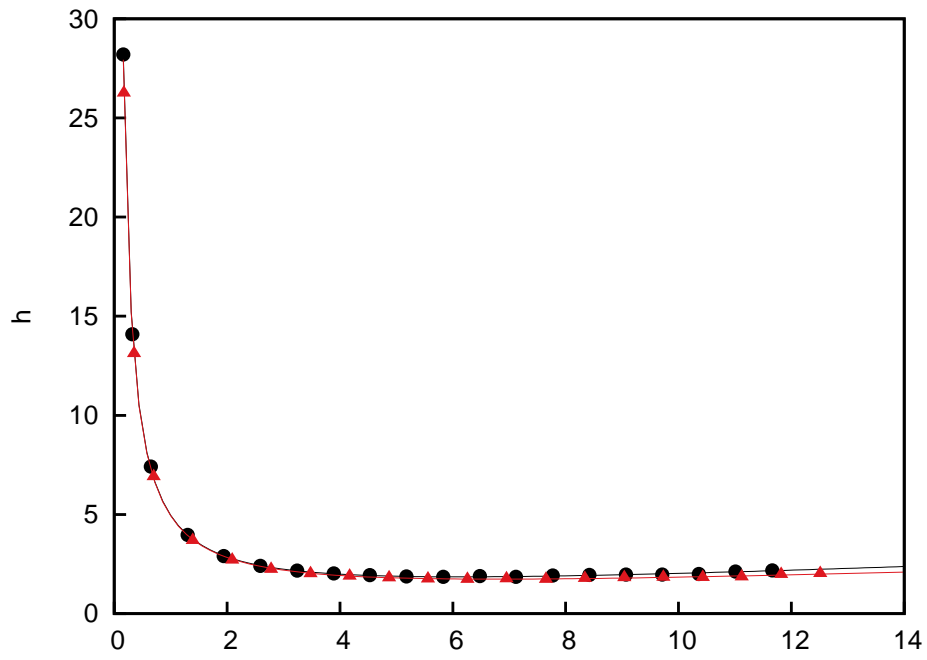


Figure 5:

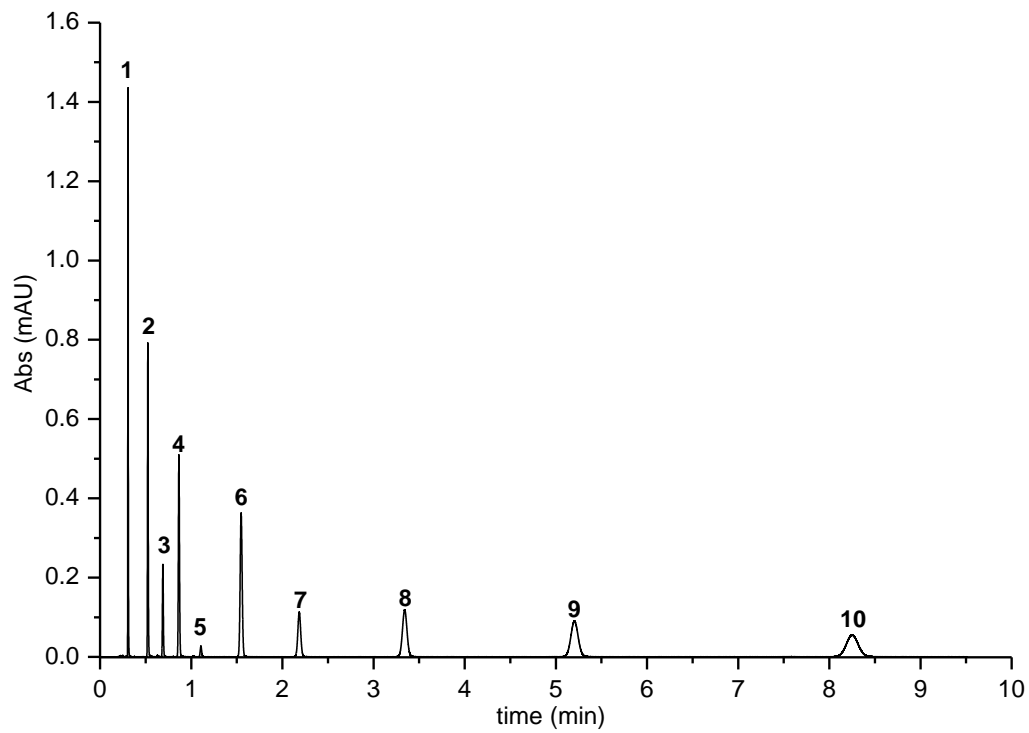


Figure 7:

Table 1: Geometrical characteristics and physico-chemical properties of the Titan C₁₈ columns: total (ϵ_t), interstitial (ϵ_e) and particle (ϵ_p) porosities; specific permeability (k_0); Kozeny-Carman constants (K_c). Batch: number of silica batch. Calculation of K_c (eq. 6) for the Titan C₁₈ columns was based on d_{Sauter} . See text for further details.

L×I.D.(mm)	Batch	ϵ_t	ϵ_e	ϵ_p	$k_0 \times 10^{11}$ (cm ²)	K_c
100×3.0	8202	0.593	0.364	0.360	2.77	179
75×3.0	8033	0.613	0.381	0.375	3.06	196
50×3.0	412502	0.594	0.363	0.363	3.05	161
100×2.1	8033	0.612	0.384	0.370	3.17	196
75×2.1	7988	0.600	0.370	0.365	3.38	157
50×2.1	412502	0.605	0.366	0.377	3.05	166

Table 2: Bulk molecular diffusion coefficient, D_m , estimated through peak parking measurements for the four compounds considered in this work. Mobile phase: ACN/water 60/40 v/v; T: 35°C

Compound	$D_m \times 10^5$ (cm ² /s)
Nitrobenzene	1.92
Toluene	2.10
Ethylbenzene	1.88
Butylbenzene	1.76

References

- [1] F. Gritti, G. Guiochon, Perspectives on the evolution of the column efficiency in liquid chromatography, *Anal. Chem.* 85 (2013) 3017–3035.
- [2] K. Broeckhoven, G. Desmet, The future of UHPLC: towards higher pressure and/or smaller particles?, *Trends Anal. Chem.* 63 (2014) 65–75.
- [3] J. Kirkland, J. DeStefano, The art and science of forming packed analytical high-performance liquid chromatography columns, *J. Chromatogr. A* 1126 (2006) 50– 57.
- [4] Development of a New Monodisperse Porous Silica for UHPLC, Poster presented at 38th International Symposium on High Performance Liquid Phase Separations and Related Technique, (HPLC 2012), June 16-21, 2012, Anaheim, CA, USA.
- [5] A. Daneyko, A. Hölzel, K. Khirevich, U. Tallarek, Influence of the particle size distribution on hydraulic permeability and eddy dispersion in bulk packings, *Anal. Chem.* 83 (2011) 3903–3910.
- [6] A. Daneyko, D. Hlushkou, S. Khirevich, U. Tallarek, From random sphere packings to regular pillar arrays: Analysis of transverse dispersion, *J. Chromatogr. A* 1257 (2012) 98 – 115.
- [7] S. Bruns, D. Stoeckel, B. M. Smarsly, U. Tallarek, Influence of particle properties on the wall region in packed capillaries, *J. Chromatogr. A* 1268 (2012) 53 – 63.
- [8] S. Bruns, E. G. Franklin, J. P. Grinias, J. M. Godinho, J. W. Jorgenson, U. Tallarek, Slurry concentration effects on the bed morphology and separation efficiency of capillaries packed with sub-2 μ m particles, *J. Chromatogr. A* 1318 (2013) 189 – 197.
- [9] F. Gritti, D. S. Bell, G. Guiochon, Particle size distribution and column efficiency. An ongoing debate revived with 1.9 μ m Titan-C₁₈ particles, *J. Chromatogr. A* 1355 (2014) 179–192.

- [10] F. Gritti, G. Guiochon, The rationale for the optimum efficiency of columns packed with new $1.9\mu\text{m}$ fully porous Titan- C_{18} particles. A detailed investigation of the intra-particle diffusivity, *J. Chromatogr. A* 1355 (2014) 164–178.
- 330 [11] J. W. Thompson, R. A. Lieberman, J. W. Jorgenson, Hydrodynamic chromatography for the size classification of micron and sub-micron sized packing materials, *J. Chromatogr. A* 1216 (2009) 7732 – 7738.
- [12] U. D. Neue, *HPLC Columns: Theory, Technology and Practice*, Wiley-VCH, 1997.
- [13] F. Gritti, G. Guiochon, Mass transfer kinetics, band broadening and column efficiency, 335 *J. Chromatogr. A* 1221 (2012) 2–40.
- [14] J. C. Giddings, *Dynamics of Chromatography*, Marcel Dekker, New York, 1965.
- [15] A. de Villiers, H. Lauer, R. Szucs, S. Goodall, P. Sandra, Influence of frictional heating on temperature gradients in ultra-high-pressure liquid chromatography on 2.1 mm i.d. columns, *J. Chromatogr. A* 1113 (2006) 84–91.
- 340 [16] D. Åsberg, J. Samuelsson, M. Lesko, A. Cavazzini, K. Kaczmarek, T. Fornstedt, Method transfer from high-pressure liquid chromatography to ultra-high-pressure liquid chromatography. II. Temperature and pressure effects, *J. Chromatogr. A* 1401 (2015) 52–59.
- [17] I. Halász, K. Martin, Pore Size of Solids, *Angew. Chem. Int. Ed. Engl* 17 (1978) 901–908.
- [18] A. Felinger, *Data analysis and signal processing in chromatography*, Elsevier, Amsterdam, 1998. 345
- [19] F. Gritti, G. Guiochon, A protocol for the measurement of all the parameters of the mass transfer kinetics in columns used in liquid chromatography, *J. Chromatogr. A* 1217 (2010) 5137–5151.
- [20] D. Cabooter, J. Billen, H. Terryn, F. Lynen, P. Sandra, G. Desmet, Detailed characterisation of the flow resistance of commercial sub- $2\mu\text{m}$ reversed-phase columns, 350 *J. Chromatogr. A* 1178 (2008) 108–117.

- [21] J. H. Knox, R. Kaliszan, Theory of solvent disturbance peaks and experimental determination of thermodynamic dead-volume in column liquid chromatography, *J. Chromatogr.* 349 (1985) 211–234.
- 355 [22] G. Guiochon, A. Felinger, D. G. Shirazi, A. M. Katti, *Fundamentals of Preparative and Nonlinear Chromatography*, Academic Press, Elsevier, Second Edition, 2006.
- [23] J. H. Knox, L. McLaren, New gas chromatographic method for measuring gaseous diffusion coefficients and obstructive factors, *Anal. Chem.* 36 (1964) 1477–1482.
- [24] K. Miyabe, Y. Matsumoto, G. Guiochon, Peak parking-moment analysis. A strategy for
360 the study of the mass-transfer kinetics in the stationary phase, *Anal. Chem.* 79 (2007) 1970–1982.
- [25] D. Ludlum, R. Warner, H. Smith, The Diffusion of thiourea in water at 25°C, *J. Phys. Chem* 66 (1962) 1540–1542.
- [26] M. J. Rosen, J. T. Kunjappu, *Surfactants and interfacial phenomena*, Wiley & Sons,
365 Inc., Hoboken, New Jersey, USA, 2012.
- [27] S. Khirevich, A. Daneyko, A. Höltzel, A. Seidel-Morgenstern, U. Tallarek, Statistical analysis of packed beds, the origin of short-range disorder, and its impact on eddy dispersion, *J. Chromatogr. A* 1217 (2010) 4713–4722.
- [28] J. F. Richardson, J. H. Harker, J. R. Backhurst, *Coulson and Richardson’s Chemical Engineering*, 5th Edition, Vol. 2, Elsevier, Amsterdam, 2002, Ch. 4.
370
- [29] G. Desmet, D. Clicq, P. Gzil, Geometry-independent plate height representation methods for the direct comparison of the kinetic performance of LC supports with a different size morphology, *Anal. Chem.* 77 (2005) 4058–4070.